

A solar chimney power plant with a square-based pyramidal shape: theoretical considerations

Dardan Klimenta

Faculty of Technical Sciences
University of Priština in Kosovska Mitrovica
Kosovska Mitrovica, Serbia
dardan.klimenta@pr.ac.rs

Joan Peuteman

Kulab
KU Leuven
Oostende, Belgium
joan.peuteman@kuleuven.be

Jelena Klimenta

Independent consultant
in the field of urban and spatial planning
Niš, Serbia
klimenta.jelena@gmail.com

Abstract—A new model for a solar chimney power plant with a square-based pyramidal shape, having three sloped solar collectors, a chimney and a field of sun-tracking mirrors, has been considered in this paper from a theoretical point of view. The geographical latitude and the dimensions of the pyramidal base structure correspond to the ones of the Great Pyramid of Giza. The east, south and west sides of the pyramid are assumed to be constructed as flat solar collectors, while the upper part of the chimney has a cylindrical collector. According to the model, a material layer having a high heat capacity is placed below each of the absorber surfaces, while the lower surfaces of these materials are adiabatic. The upper part of the chimney of the studied solar power plant is a hollow cylindrical reservoir which mainly receives heat from the sun-tracking mirrors. A comparison between the proposed model and a prototype of the classical solar chimney power plant has been made as well.

Key Words—electricity; square-based pyramid; solar chimney; solar energy; solar power plant;

I. INTRODUCTION

A solar chimney power plant (SCPP) consists of following components: solar collectors, a chimney and a turbine-generator unit. Traditionally, a SCPP installed on a horizontal ground surface at low latitude consists of a circular transparent canopy raised at a certain height from the ground, with a chimney at its centre [1]. A SCPP installed on a sloped ground surface at high latitude consists of a sloped collector having a triangular surface area with a chimney at its apex [1]. In both cases, the chimneys house one or more turbine-generator units located at their bases [2]. The chimney is significantly shorter in the second case. Solar radiation penetrates the transparent collector cover and strikes the ground below it. The ambient air enters from the periphery of the collectors and rises, being heated by the ground, to the centre or to the apex where a vertical chimney is installed. The heated air underneath the collector flows towards and up into the chimney to drive the turbine-generator units [2].

Using a turbine-generator unit, the kinetic energy of the air flow converts into electrical energy. Three simple principles are used: the solar greenhouse effect, the chimney buoyancy effect and the wind power principle [3]. Therefore, the collector is the heat source, the chimney is the engine, and the turbine-generator group is the power conversion unit [3].

Experimental results on large scale commercial systems have never been reported since a 50 kW power prototype was built in Manzanares (Spain) in 1982 [4-6]. Among others a smaller 0.6 kW power prototype was built in Gaborone (Botswana) in 2008 as well [6]. Realizing a large scale commercial solar chimney requires financial support and due to high start-up costs and unproven technology, it is not easy to get funding [6]. That is the main reason why research on solar chimneys usually reduces to mathematical modeling of heat transfer processes. More precisely, in general the temperature and the velocity of the air [7-9] are studied. Moreover, the SCPPs still need a lot of research to make the technology viable by improving the efficiency and reducing start-up costs [6].

A SCPP installed on a horizontal ground surface at low latitude containing three sloped solar collectors, each having the shape of a trapezium, with a chimney at their upper bases is considered in this paper. The collectors cover the east, south and west sides of a pyramidal base structure having the same dimensions of the Great Pyramid of Giza. On the north side, the truncated pyramid has one inlet implying there is no collector on this north side. The ambient air enters the pyramid from the north side and drops to the ground surface as cooled by the pyramid's interior where three side-outlets are left (on the east, south and west sides). There is a large mass of stone inside the pyramid implying the interior air temperature is constant and equals $T_{a,i}=20\text{ }^{\circ}\text{C}$ [10]. The height of the truncated pyramid equals $H_{TP}=142.018\text{ m}$. The chimney has a height $H_{SC}=52.582\text{ m}$ and an inner diameter $d_{SC}=10.16\text{ m}$ [11]. The upper part of the chimney has a length $L_{CC}=10\text{ m}$ and is

designed as a hollow cylindrical reservoir having an inner surface temperature $T_{CC}=565\text{ }^{\circ}\text{C}$ [12]. The SCPP uses a large field of rotating mirrors to track the Sun and focus the reflected sunlight onto a heat-receiving upper part of the chimney. The fluid in the reservoir collects the heat and uses it to warm up the air inside the chimney.

In the present paper, the authors suggest the use of a mathematical model being a combination of the theoretical model given in [13], existing empirical correlations (for radiation, for natural convection, for forced convection, for sky temperature and for air velocity inside the chimney) and new correlations for natural convection along an inclined flat plate/surface. In order to make these new results comparable with existing ones, the total height of the SCPP is assumed to equal the height of the prototype which has been built in Manzanares. The other ambient conditions correspond to the climate in Giza.

II. DESIGN AND CONSTRUCTION OF A NEW SCPP

In an ideal situation, the absorber surface (or flat solar collector) is inclined at an angle which equals the local latitude implying the absorber surface will be exposed to maximum solar radiation throughout the whole year [14,15]. As the considered site is located in Giza and the latitude of the Great Pyramid equals $29^{\circ}58'51''\text{N}$, the inclination angle ought to be 29.981° facing the south in this case. However, the inclination angles of the sides of the Great Pyramid equal $\gamma=51.844^{\circ}$ [16] and approximates the sum of the angle of local latitude and the angle of the Earth's axial inclination (23.44°) on the summer solstice. By choosing this angle of the sides of the Great Pyramid vs. its latitude, the pyramid casts no shadow at noon during the spring equinox. Moreover, the natural draft forces created in the trapezoidal ducts between the transparent covers and the absorber surfaces are significantly higher. Accordingly, the Sun's position in relation to a SCPP throughout a day at north latitude is shown in Fig. 1.

Two typical cross-sections of the proposed SCPP design are presented in Figs. 2 and 3. A north to south cross-section of the SCPP is shown in Fig. 2, while a west to east one is shown in Fig. 3. It is assumed that the system of chambers, galleries and tunnels, which is similar to the existing one from the Great Pyramid, may provide the interior air temperature of $20\text{ }^{\circ}\text{C}$.

The depth of the trapezoidal air ducts is considered to be $\Delta_D=0.3\text{ m}$ (and $\Delta_D=0.6\text{ m}$), while the thickness of the material with a high heat capacity is considered to be $\Delta_M=\Delta_D$. Moreover, it is assumed that: (i) the material with a high heat capacity is magnesite (brick) having a thermal conductivity $k_f=3.8\text{ W}\cdot\text{m}^{-1}\cdot\text{K}^{-1}$, a density $\rho=3010\text{ kg}\cdot\text{m}^{-3}$, and a specific heat $c_p=1130\text{ J}\cdot\text{kg}^{-1}\cdot\text{K}^{-1}$ [17]; (ii) the absorber surface is painted with no-shiny black paint in order to increase its absorption of solar radiation and to increase its temperature [14]; (iii) the transparent cover is a $\Delta_C=0.005\text{ m}$ thick acrylic plate having a thermal conductivity $k_{t,C}=0.19\text{ W}\cdot\text{m}^{-1}\cdot\text{K}^{-1}$ [14]; and (iv) the trapezoidal ducts of the east, south and west solar collectors are mutually separated.

The main difference between the proposed SCPP design and the existing models originates from the cooling system for

the ambient air. The applications which have been modeled in the past use ambient air entering the SCPP from the periphery implying a non-constant temperature throughout the whole year. In the present model, the air first passes through the pyramid interior implying it has a constant temperature before the heating process starts.

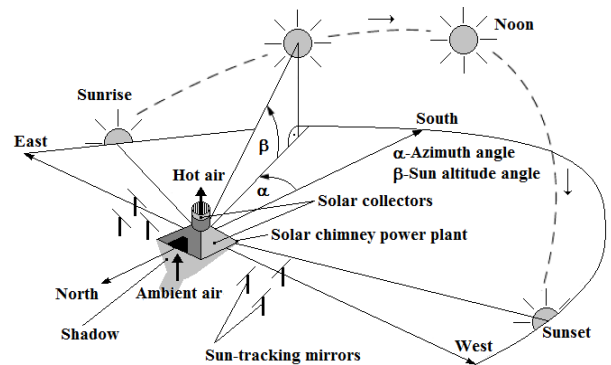


Figure 1. The Sun's position in relation to the SCPP throughout a day at north latitude.

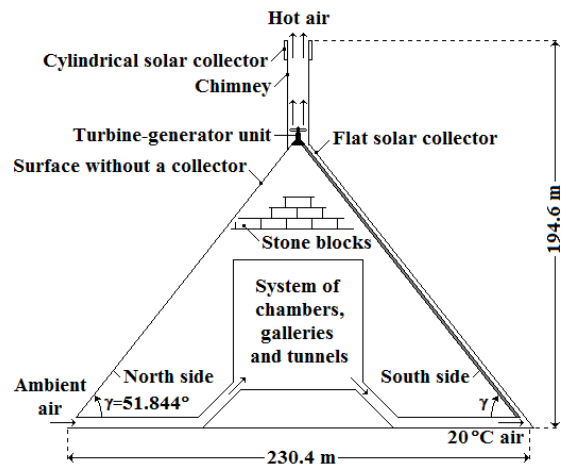


Figure 2. A north to south cross-section of the SCPP.

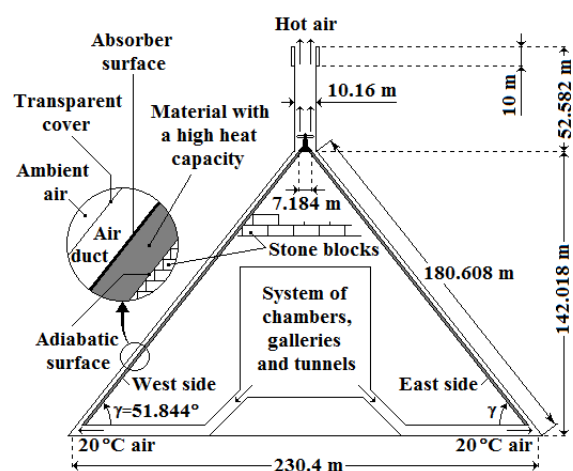


Figure 3. A west to east cross-section of the SCPP.

III. MATHEMATICAL MODEL

A mathematical model based on the law of energy conservation has been formulated to predict the performance of the SCPP described in the previous section. The heat transfer processes in the three trapezoidal air ducts are considered. Moreover, the natural draft induced by the solar chimney and by the cylindrical solar collector is included in the model. However, the present study mainly focuses on the solar chimney effect.

When modeling natural draft in the proposed SCPP, it is important to determine the air flow rate which can be handled under particular operating conditions. The mathematical model is based on the following assumptions: (i) steady-state conditions are considered and end effects are neglected; (ii) a non-uniform heating of the collector surfaces depending on the altitude angle of the Sun is neglected [8]; (iii) the flows in the trapezoidal ducts are considered to be flows between two parallel flat plates [8]; (iv) the side collectors are placed over inclined flat surfaces; (v) the heat losses through the wall of the chimney are neglected [8]; (vi) the material with a high heat capacity is considered as "a fully charged heat capacity", i.e. the heat losses through the absorber surface are neglected; (vii) all sides of the pyramid covered by the collectors have the same operating conditions; (viii) the air satisfies the ideal gas law [18]; (ix) no air leakage occurs through the covers or along the edges of the covers; (x) only the buoyancy force is considered, i.e. natural draft induced by wind is not included [18]; and (xi) in a number of simulations, the upper part of the chimney is considered as an isothermal surface having a surface temperature $T_{CC}=565\text{ }^{\circ}\text{C}$.

An energy balance model for computing the air flow parameters is shown in Fig. 4. The parameters displayed in Fig. 4 have the following meanings: n is a normal to the upward-facing surface of the transparent cover; γ is the angle between the vertical and the normal n ; ψ is the angle of inclination from the vertical; $\delta=10.491^{\circ}$ is the angle between the sunrays and the normal n ; g is the gravitational constant; Δ_C , Δ_D and Δ_M are the thicknesses of the transparent cover, the trapezoidal duct and the material with a high heat capacity, respectively; H_{SC} is the height of the chimney; L_{CC} is the length of the cylindrical solar collector; T_{CC} , T_{Cu} , T_{Cd} and T_A , are the temperatures of the cylindrical solar collector, the upward-facing cover surface, the downward-facing cover surface and the absorber surface (adiabatic surface), respectively; T_a , $T_{a,i}$, $T_{a,o}$, and T_{sky} are the temperatures of the ambient air, the air at the inlet of the trapezoidal duct, the air at the outlet of the trapezoidal duct and the sky, respectively; $T_{a,avg}$ and T_C are the average temperatures of the air in the trapezoidal duct and the transparent cover, respectively; $v_{a,i}$ and $v_{a,o}$ are the velocities of the air at the inlet and at the outlet of the trapezoidal duct, respectively; $\alpha_A=0.9$ is the absorption coefficient of the absorber surface; $\tau_C=0.91$ is the transmittance coefficient of the transparent cover; $Q'_{E,s,S}$ is the solar irradiance on the transparent cover which is not oriented perpendicularly to the sunrays; $Q_{E,s,S}=Q'_{E,s,S}\cdot\cos\delta$ is the solar irradiance component which is perpendicular to the absorber surface; $\alpha_A\cdot\tau_C\cdot Q_{E,s,S}$ is the amount of solar radiation absorbed by the absorber surface per second; $Q_{air,i-o}$ is the amount of heat absorbed by the inside air per second; $Q_{t,s,C}$ is

the amount of heat lost due to radiation, convection and conduction through the transparent cover per second; $Q_{th,s,CC}$ is the amount of heat exchanged by convection between the internal surface of the cylindrical collector and the inside air per second. For all the earlier mentioned parameters, the SI unit system has been selected as default.

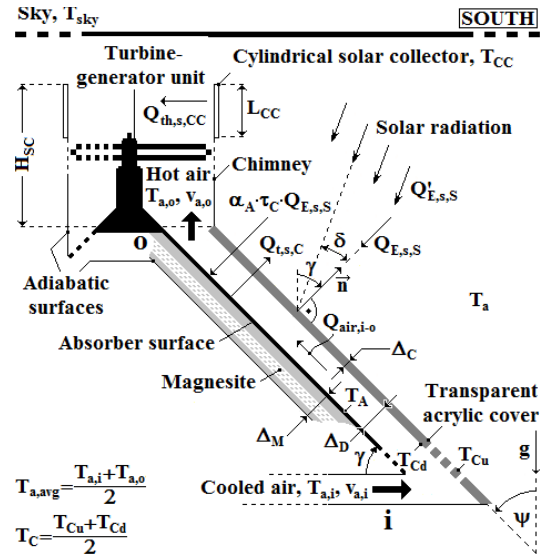


Figure 4. Energy balance model for computing the air flow parameters.

The air flow rate in the SCPP is a complex function of design and operating parameters such as geometry, local latitude, orientation, altitude angle of the Sun, solar irradiance, ambient temperature, etc. The chimney, three sloped collectors and one cylindrical collector induce day air draft. Internal and external heat capacities/storages can also induce night air draft. The total air flow rate in the chimney ($\dot{m}_{a,t}$) is the sum of air flow rates in the trapezoidal ducts ($3 \cdot \dot{m}_{a,d}$), i.e.

$$\begin{aligned} \dot{m}_{a,t} &= \rho'_i \cdot v'_{a,i} \cdot S'_D = \rho'_o \cdot v'_{a,o} \cdot S'_D = \\ &= 3 \cdot \dot{m}_{a,d} = 3 \cdot \rho_i \cdot v_{a,i} \cdot S_{D,i} = 3 \cdot \rho_o \cdot v_{a,o} \cdot S_{D,o} \end{aligned} \quad (1)$$

where $v'_{a,i}$ and $v'_{a,o}$ are the velocities of the air at the inlet and at the outlet of the chimney, respectively; ρ'_i and ρ'_o are the air densities corresponding to $T'_{a,i}=T_{a,o}$ and $T'_{a,o}=(T_{a,o}+T_{CC})/2$, respectively; $S'_D=81.073\text{ m}^2$ is the cross-sectional area of the chimney duct; ρ_i and ρ_o are the air densities corresponding to $T_{a,i}$ and $T_{a,o}$, respectively; and $S_{D,i}=213.12\text{ m}^2$ (and $S_{D,i}=426.24\text{ m}^2$) and $S_{D,o}=6.6452\text{ m}^2$ (and $S_{D,o}=13.2904\text{ m}^2$) are the cross-sectional areas of the trapezoidal duct at the inlet and at the outlet, respectively. The term $\dot{m}_{a,d}$, however, is lower during night time operation. The night air draft is mainly created by the cylindrical collector using heat stored during day time.

The heat transfer coefficients corresponding to the heat transfer processes $Q_{t,s,C}$ and $Q_{th,s,CC}$ are $h_{U,C}$ and h_{CC} , respectively. When a number of the parameters given in Fig. 4 are known, the temperature of the air at the outlet of the trapezoidal duct as well as heat losses due to convection and radiation need to be estimated.

The iterative procedure for computing $T_{a,o}$ requires knowledge of $v_{a,i}$, $v_{a,o}$, $v'_{a,i}$, $v'_{a,o}$, h_{CC} , $h_{U,C}$, h_A , $h_{r,A}$, T_A , T_C and T_{sky} , which are initially unknown. To obtain an initial estimate of $T_{a,o}$, the same numerical values for the heat transfer coefficients (for example $12 \text{ W}\cdot\text{m}^{-2}\cdot\text{K}^{-1}$) and the air velocities (for example $1 \text{ m}\cdot\text{s}^{-1}$) can be taken for all unknown heat transfer coefficients and velocities, respectively. Therefore, an initial estimate of $T_{a,o}$ can be made from

$$\alpha_A \cdot \tau_C \cdot Q_{E,s,S} \cdot S_C + Q_{th,s,CC} \cdot S_{CC} / 3 = Q_{air,i-o} + Q_{t,s,C} \cdot S_C \quad (2)$$

as follows

$$T_{a,o} = \frac{\left[6 \cdot \alpha_A \cdot \tau_C \cdot Q_{E,s,S} \cdot S_C + 6 \cdot v_{a,o} \cdot \rho_o \cdot S_{D,o} \cdot c_{p,i} \cdot T_{a,i} + \right.}{\left. 6 \cdot v_{a,o} \cdot \rho_o \cdot S_{D,o} \cdot c_{p,i} + 3 \cdot h_{U,C} \cdot S_C + 2 \cdot h_{CC} \cdot S_{CC} \right]} \quad (3)$$

where [7,13,14]

$$Q_{th,s,CC} = h_{CC} \cdot (T_{CC} - T_{a,o}) \quad (4)$$

$$h_{CC} = 5.7 + 3.8 \cdot v'_{a,avg} \quad (5)$$

$$Q_{air,i-o} = v_{a,o} \cdot \rho_o \cdot S_{D,o} \cdot c_{p,i} \cdot (T_{a,o} - T_{a,i}) \quad (6)$$

$$Q_{t,s,C} = h_{U,C} \cdot (T_{a,avg} - T_a) \quad (7)$$

$$h_{U,C} = \left(\frac{1}{h_{Cd} + h_{r,Cd}} + \frac{\Delta_C}{k_{t,C}} + \frac{1}{h_{Cu} + h_{r,Cu}} \right)^{-1} \quad (8)$$

$$h_{r,Cd} = \frac{\sigma_{SB}}{1/\epsilon_A + 1/\epsilon_C - 1} \cdot \frac{T_A^4 - T_C^4}{T_{a,avg} - T_C} \quad (9)$$

$$h_{r,Cu} = \epsilon_C \cdot \sigma_{SB} \cdot (T_C^4 - T_{sky}^4) / (T_C - T_a) \quad (10)$$

$$T_A = \frac{\alpha_A \cdot \tau_C \cdot Q_{E,s,S} \cdot S_C - Q_{air,i-o}}{(h_A + h_{r,A}) \cdot S_C} + T_{a,avg} \quad (11)$$

$$h_{r,A} = \frac{\sigma_{SB}}{1/\epsilon_A + 1/\epsilon_C - 1} \cdot \frac{T_A^4 - T_C^4}{T_a - T_{a,avg}} \quad (12)$$

$$T_C \approx (T_{a,avg} + T_a) / 2 \quad (13)$$

$$T_{sky} = 0.0552 \cdot T_a^{1.5} \quad (14)$$

$S_C=21454.786 \text{ m}^2$ is the surface area of one transparent cover; $S_{CC}=\pi \cdot d_{SC} \cdot L_{CC}=319.186 \text{ m}^2$ is the inner surface area of the cylindrical solar collector; $c_{p,i}$ is the specific heat of the air at temperature $T_{a,i}$; $v'_{a,avg}=(v'_{a,i}+v'_{a,o})/2$ is the average velocity of the air in the chimney duct; h_{Cd} and $h_{r,Cd}$ are the heat transfer coefficients for forced convection and radiation between the inside air and the downward-facing surface of the transparent cover, respectively; h_{Cu} and $h_{r,Cu}$ are the heat transfer coefficients for natural convection and radiation between the upward-facing surface of the transparent cover and the ambient air, respectively; h_A and $h_{r,A}$ are the heat transfer coefficients for forced convection and radiation between the absorber surface and the inside air, respectively; $\epsilon_A=0.96$ is the thermal

emission coefficient of the absorber surface; $\epsilon_C=0.94$ is the thermal emission coefficient of the transparent cover; and σ_{SB} is the Stefan-Boltzmann constant.

Five temperature dependent parameters for air at temperature T_f taking the value T_a , $T_{a,i}$, $T_{a,o}$, $T'_{a,o}$ or $T_{a,avg}$ are used: density ρ , specific heat c_p , dynamic viscosity μ , thermal conductivity k_t and Prandtl number Pr . These parameters have been read from corresponding input data files and interpolated using a cubic spline. The kinematic viscosity, the thermal diffusivity and the thermal expansion coefficient of air are taken as $\nu=\mu/\rho$, $\alpha_t=k_t/(\rho \cdot c_p)$ and $\beta=1/T_f$, respectively. Thus, the Rayleigh number based on the height of the transparent cover can be expressed as

$$Ra = \frac{g \cdot \beta}{\nu \cdot \alpha_t} \cdot (T_C - T_a) \cdot L_C^3 \quad (15)$$

where $L_C=180.608 \text{ m}$ is an appropriate characteristic length.

A Nusselt number correlation for natural convection along a flat plate inclined at an angle $0<\psi<90^\circ$ equals

$$Nu = C \cdot [Ra / (1 + 0.492 / Pr)]^n \quad (16)$$

where $C=0.67 \cdot (\cos\psi)^n$ and $n=1/4$ for a laminar flow ($Gr \leq Gr_{cr}$), $C=0.155 \cdot (\sin\psi)^n$ and $n=1/3$ for a turbulent flow ($Gr > Gr_{cr}$). Here, Gr is the Grashof number, and Gr_{cr} is the critical Grashof number that can be computed from $\log_{10}(Gr_{cr} \cdot Pr) = 5 \cdot \cos\psi + 3.65$ [19]. In case of a laminar flow, the coefficients C and n are determined based on empirical correlations from [17,20]. In case of a turbulent flow, the coefficients C and n are correlated using experimental results from [21]. This implies the heat transfer coefficient h_{Cu} equals $h_{Cu} = Nu \cdot k_t / L_C$.

By equating the total pressure difference due to buoyancy (natural draft pressure) $\Delta p_{t,bouy} = g \cdot (\rho_i - \rho_o) \cdot L_C \cdot (\sin\gamma)^2 + g \cdot (\rho_o - \rho'_o) \cdot H_{SC}$ and the total pressure drop (the sum of the pressure losses due to friction of the walls, across the turbine, at the inlets and at the outlets) $\Delta p_{t,loss} = f_C \cdot L_C \cdot \rho_o \cdot (v_{a,o})^2 / (2 \cdot d_{H,avg}) + K_{i+o} \cdot \rho_o \cdot (v_{a,o})^2 / 2 + \Delta p_{turb} + f_{SC} \cdot H_{SC} \cdot \rho'_o \cdot (v'_{a,o})^2 / (2 \cdot d_{SC}) + K'_{i+o} \cdot \rho'_o \cdot (v'_{a,o})^2 / 2$, the velocity of the air at the outlet of one trapezoidal duct can be expressed as [9,18,22,23]:

$$v_{a,o} = \frac{[2 \cdot (\Delta p_{t,bouy} - \Delta p_{turb}) / \rho_o]^{1/2}}{\left[\frac{f \cdot L_C}{d_H} + K_{i+o} + \frac{9 \cdot \rho_o \cdot S_{D,o}^2}{\rho_o^2 \cdot S_D^2} \cdot \left(\frac{f' \cdot H_{SC}}{d_{SC}} + K'_{i+o} \right) \right]^{1/2}} \quad (17)$$

where Δp_{turb} is the pressure loss across the turbine which is assumed to be 0 and $(2/3) \cdot \Delta p_{t,bouy}$ [23]; f (or f') is the friction coefficient amounting to $64/Re$ and $[1.82 \cdot \log_{10}(Re) - 1.64]^2$ for laminar and turbulent flows in a smooth pipe, respectively [22]. Moreover, $Re = v_{a,avg} \cdot d_H / \nu_{avg}$ is the Reynolds number; $v_{a,avg} = (v_{a,i} + v_{a,o}) / 2$ is the average velocity of the air in the trapezoidal duct; $d_H = 1.2 \text{ m}$ (and $d_H = 2.4 \text{ m}$) is the hydraulic diameter [13]; ν_{avg} is the kinematic viscosity of the air at temperature $T_{a,avg}$; $K_{i+o} = 2.9$ is the sum of the pressure loss coefficients at inlet and outlet openings of the trapezoidal duct [9,18]; and $K'_{i+o} = 2$ is the sum of the pressure loss coefficients at inlet and outlet openings of the chimney duct [23].

Moreover, the value $T_{a,o}$ should be recomputed by averaging the assumed and found values of h_{CC} , h_{Cd} , $h_{r,Cd}$, h_{Cu} , $h_{r,Cu}$, h_A , $h_{r,A}$ and $v_{a,o}$ in each iteration. This approach must be iterated until the difference between the assumed and found $T_{a,o}$ values becomes negligibly small. Ultimately, this iterative procedure utilizes the final value of $T_{a,o}$ to evaluate the final values of h_{CC} , h_{Cd} , $h_{r,Cd}$, h_{Cu} , $h_{r,Cu}$, h_A , $h_{r,A}$ and $v_{a,o}$.

If the generator and gearbox efficiency equals $\eta_{el}=0.9$, the electric power from the SCPP becomes

$$P_{el} = \eta_{el} \cdot P_{turb} = \eta_{el} \cdot \eta_{turb} \cdot \Delta p_{turb} \cdot v'_{a,avg} \cdot S'_D \quad (18)$$

where P_{turb} is the power generated by the turbine and $\eta_{turb}=0.85$ is the turbine efficiency [1,24].

IV. RESULTS AND DISCUSSION

Fig. 5 shows that an increase in the solar irradiance causes an efficiency drop of the sloped solar collectors. The collector efficiency η_{coll} is defined according to [24]. Moreover, the proposed model suggests that as the solar irradiance increases the temperature difference between the air at the outlet and at the inlet of a trapezoidal duct ($T_{a,o}-T_{a,i}$) increases. This dependency is presented in Fig. 5 as well. The maximum collector efficiency is achieved with $\Delta_c=0.6$ m and without a turbine in the chimney. The maximum temperature difference is achieved with $\Delta_c=0.3$ m and with a turbine. The ambient air temperature was $T_a=34$ °C.

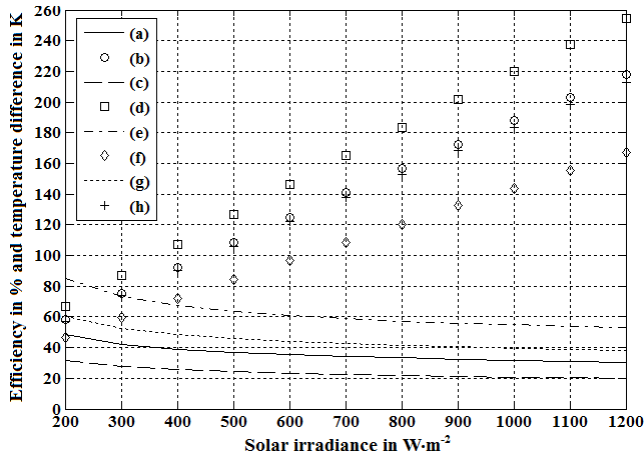


Figure 5. Collector efficiency η_{coll} and temperature difference ($T_{a,o}-T_{a,i}$) with respect to the solar irradiance $Q_{E,S,S}$: (a) η_{coll} for $\Delta_c=0.3$ m and $\Delta p_{turb}=0$ Pa; (b) ($T_{a,o}-T_{a,i}$) for $\Delta_c=0.3$ m and $\Delta p_{turb}=0$ Pa; (c) η_{coll} for $\Delta_c=0.3$ m and $\Delta p_{turb}=(2/3) \cdot \Delta p_{t,bouy}$; (d) ($T_{a,o}-T_{a,i}$) for $\Delta_c=0.3$ m and $\Delta p_{turb}=(2/3) \cdot \Delta p_{t,bouy}$; (e) η_{coll} for $\Delta_c=0.6$ m and $\Delta p_{turb}=0$ Pa; (f) ($T_{a,o}-T_{a,i}$) for $\Delta_c=0.6$ m and $\Delta p_{turb}=0$ Pa; (g) η_{coll} for $\Delta_c=0.6$ m and $\Delta p_{turb}=(2/3) \cdot \Delta p_{t,bouy}$; (h) ($T_{a,o}-T_{a,i}$) for $\Delta_c=0.6$ m and $\Delta p_{turb}=(2/3) \cdot \Delta p_{t,bouy}$.

Fig. 6 gives information about the outlet air velocities that could be achieved in the trapezoidal ducts and in the chimney with the solar irradiance starting from $200 \text{ W}\cdot\text{m}^{-2}$ and increasing to $1200 \text{ W}\cdot\text{m}^{-2}$. The air velocities $v_{a,o}$ and $v'_{a,o}$ for two different depths of the trapezoidal air ducts are calculated. As expected, the air velocities due to natural draft will increase as the solar irradiance increases.

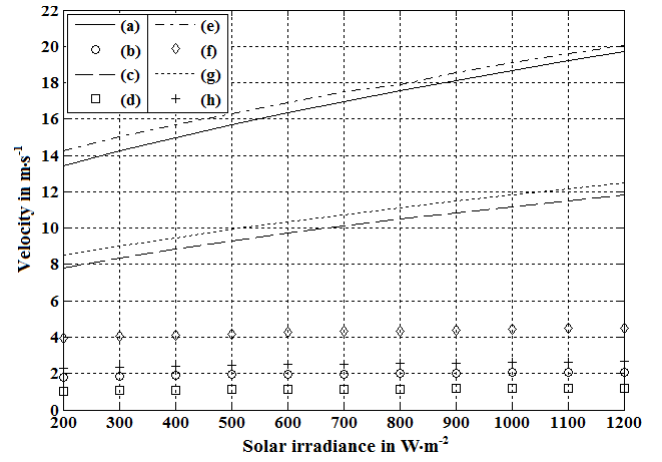


Figure 6. Air velocities $v_{a,o}$ and $v'_{a,o}$ with respect to the solar irradiance $Q_{E,S,S}$: (a) $v_{a,o}$ for $\Delta_c=0.3$ m and $\Delta p_{turb}=0$ Pa; (b) $v'_{a,o}$ for $\Delta_c=0.3$ m and $\Delta p_{turb}=0$ Pa; (c) $v_{a,o}$ for $\Delta_c=0.3$ m and $\Delta p_{turb}=(2/3) \cdot \Delta p_{t,bouy}$; (d) $v'_{a,o}$ for $\Delta_c=0.3$ m and $\Delta p_{turb}=(2/3) \cdot \Delta p_{t,bouy}$; (e) $v_{a,o}$ for $\Delta_c=0.6$ m and $\Delta p_{turb}=0$ Pa; (f) $v'_{a,o}$ for $\Delta_c=0.6$ m and $\Delta p_{turb}=0$ Pa; (g) $v_{a,o}$ for $\Delta_c=0.6$ m and $\Delta p_{turb}=(2/3) \cdot \Delta p_{t,bouy}$; (h) $v'_{a,o}$ for $\Delta_c=0.6$ m and $\Delta p_{turb}=(2/3) \cdot \Delta p_{t,bouy}$.

In Fig. 7, the electric power generated by a turbine-generator unit P_{el} and the pressure drop across the turbine Δp_{turb} are plotted against the solar irradiance $Q_{E,S,S}$. The electric power and the pressure drop across the turbine increase as the solar irradiance increases. Moreover, by increasing the depths of the trapezoidal air ducts from 0.3 m to 0.6 m, the electric power increases more than twice.

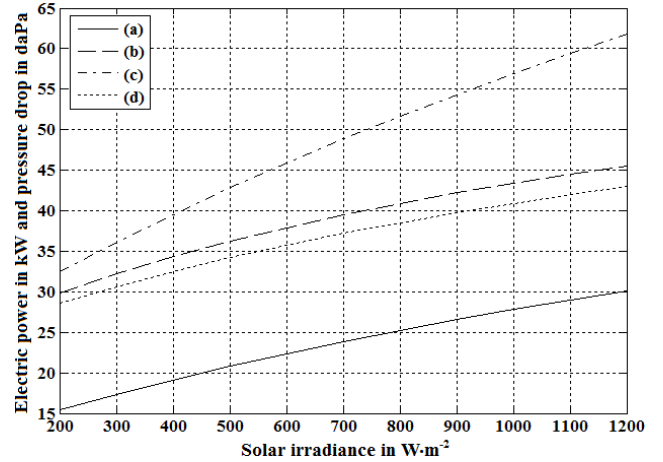


Figure 7. Electric power P_{el} and pressure drop $\Delta p_{turb}=(2/3) \cdot \Delta p_{t,bouy}$ with regard to the solar irradiance $Q_{E,S,S}$: (a) P_{el} for $\Delta_c=0.3$ m; (b) Δp_{turb} for $\Delta_c=0.3$ m; (c) P_{el} for $\Delta_c=0.6$ m; (d) Δp_{turb} for $\Delta_c=0.6$ m.

V. CONCLUSIONS

The most important conclusions arising from this paper are:

- An increase in the air mass obtained by increasing the depth of the trapezoidal air ducts increases the efficiency of a sloped solar collector, the temperature difference between the air at the outlet and at the inlet of a trapezoidal duct, the air velocities at the outlets of

the trapezoidal and chimney ducts, and the electric power generated by the turbine-generator unit.

- Irrespective of the depth of the trapezoidal air ducts, the presence of a turbine increases the temperature difference between the air at the outlets and at the inlets of the trapezoidal ducts.
- The cross-sectional area of the chimney must be adjusted to the cross-sectional areas of the trapezoidal ducts in order to achieve the best performance of the SCPP.
- The humidity of the air inside the pyramid must be increased in order to obtain a working fluid mass which is greater than the mass of dry air.
- In comparison with the SCPP prototype at Manzanares which had a collector efficiency between 23.6 and 27.1 % for the solar irradiance of 455.6-850 W·m⁻² [24], the proposed SCPP model has collector efficiencies between 24.9 and 21.6 % for $\Delta_c=0.3$ m and between 46.9 and 41 % for $\Delta_c=0.6$ m under similar operating conditions.
- Comparing to the prototype at Manzanares which had a temperature difference between the air at the outlet and at the inlet of the solar collector ($T_{a,o}-T_{a,i}$)=11.3-17.8 K for $Q_{E,S}=455.6-850$ W·m⁻² [24], the proposed SCPP model has temperature differences between 118.07 and 192.62 K for $\Delta_c=0.3$ m and between 98.99 and 160.66 K for $\Delta_c=0.6$ m under similar operating conditions.
- The simulation results suggest that a solar irradiance $Q_{E,S}=700-800$ W·m⁻² and a trapezoidal air duct depth $\Delta_c=0.6$ m would be sufficient to achieve the electric power generated in Manzanares.

REFERENCES

- [1] E. Bilgen, and J. Rheault, "Solar chimney power plants for high latitudes", *Solar Energy*, Vol. 79, Issue 5, pp. 449-458, 2005.
- [2] J. P. Pretorius, and D. G. Kröger, "Critical evaluation of solar chimney power plant performance", *Solar Energy*, Vol. 80, Issue 5, pp. 535-544, 2006.
- [3] F. Cao, H. Li, L. Zhao, T. Bao, and L. Guo, "Design and simulation of the solar chimney power plants with TRNSYS", *Solar Energy*, Vol. 98, Part A, pp. 23-33, 2013.
- [4] W. Haaf, K. Friedrich, G. Mayr, and J. Schlaich, "Solar chimneys, Part I: Principle and construction of the pilot plant in Manzanares", *Solar Energy*, Vol. 2, Issue 1, pp. 3-20, 1983.
- [5] W. Haaf, "Solar chimneys, Part II: Preliminary test result from the pilot plant in Manzanares", *Solar Energy*, Vol. 2, Issue 2, pp. 141-161, 1984.
- [6] O. Motsamai, L. Bafetanye, K. Mashaba, and O. Kgaswane, "Experimental investigation of solar chimney power plant", *Journal of Energy and Power Engineering*, Vol. 7, pp. 1980-1984, 2013.
- [7] K. S. Ong, "A mathematical model of a solar chimney", *Renewable Energy*, Vol. 28, Issue 7, pp. 1047-1060, 2003.
- [8] M. A. dos S. Bernardes, A. Voß, and G. Weinrebe, "Thermal and technical analyses of solar chimneys", *Solar Energy*, Vol. 75, Issue 6, pp. 511-524, 2003.
- [9] E. P. Sakonidou, T. D. Karapantsios, A. I. Balouktsis, and D. Chassapis, "Modeling of the optimum tilt of a solar chimney for maximum air flow", *Solar Energy*, Vol. 82, Issue 1, pp. 80-94, 2008.

- [10] F. A. P. Barnard, "The imaginary metrological system of the Great Pyramid of Gizeh", John Wiley & Sons, NY, 1884.
- [11] H. F. Fasel, F. Meng, E. Shams, and A. Gross, "CFD analysis for solar chimney power plants", *Solar Energy*, Vol. 98, Part A, pp. 12-22, 2013.
- [12] R. Moore, M. Vernon, C. K. Ho, N. P. Siegel, and G. J. Kolb, "Design considerations for concentrating solar power tower systems employing molten salt", Sandia National Laboratories, SANDIA REPORT, SAND2010-6978, pp. 1-51, 2010.
- [13] D. Klimenta, B. Perović, J. Klimenta, and M. Jevtić, "Passive cooling of PV panels: The case of PV panels and solar chimneys integrated in the roof of a family house", XIII International Scientific-Professional Symposium INFOTEH – Jahorina 2014, Vol. 13, March 19-21, 2014.
- [14] A. Date, R. Singh, A. Date, and A. Akbarzadeh, "Cooling of solar cells by chimney-induced natural draft of air", *Solar2010, the 48th AuSES Annual Conference*, Canberra, ACT, Australia, December 1-3, 2010.
- [15] D. C. Larson, and C. R. Acquista, "Solar elevation angle probability distribution", *Solar Energy*, Vol. 24, Issue 4, pp. 417-420, 1980.
- [16] R. Herz-Fischler, "The shape of the Great Pyramid", Wilfrid Laurier University Press, Waterloo, Ontario, 2000.
- [17] V. S. Arpaci, A. Selamet, and S.-H. Kao, "Introduction to heat transfer", Prentice Hall Inc., NJ, 2000.
- [18] Y. J. Dai, K. Sumathy, R. Z. Wang, and Y. G. Li, "Enhancement of natural ventilation in a solar house with a solar chimney and a solid adsorption cooling cavity", *Solar Energy*, Vol. 74, Issue 1, pp. 65-75, 2003.
- [19] M. Corcione, E. Habib, and A. Campo, "Natural convection from inclined plates to gases and liquids when both sides are uniformly heated at the same temperature", *International Journal of Thermal Sciences*, Vol. 50, Issue 8, pp. 1405-1416, 2011.
- [20] W. H. McAdams, "Heat transmission", McGraw-Hill Inc., NY, 1954.
- [21] C.-K. Lim, J.-H. Heo, and B.-J. Chung, "Natural convection heat transfer on inclined plates", *Transactions of the KSME B*, Vol. 35, Issue 7, pp. 701-708, 2011.
- [22] J. P. Holman, "Heat transfer", McGraw-Hill Inc., NY, 1999.
- [23] T. W. von Backström, and A. J. Gannon, "The solar chimney air standard thermodynamic cycle", *R&D Journal*, Vol. 16, Issue 1, pp. 16-24, 2000.
- [24] A. Koonsrisuk, and T. Chitsomboon, "Mathematical modeling of solar chimney power plants", *Energy*, Vol. 51, pp. 314-322, 2013.

SADRŽAJ

U ovom radu je teorijski razmatran novi model za solarnu dimnjačku elektranu oblika piramide sa kvadratnom osnovom, tri iskošena solarna kolektora, dimnjakom i poljem rotirajućih ogledala. Pretpostavlja se da geografska širina i dimenzije piramidalne osnove odgovaraju položaju i dimenzijama Keopsove piramide u Gizi. Za istočnu, južnu i zapadnu stranu piramide se pretpostavlja da su izvedene kao ravni, dok se za gornji deo dimnjaka pretpostavlja da je izveden kao cilindrični kolektor solarnog zračenja. Saglasno modelu, ispod svake apsorpcione površine se nalazi sloj materijala sa visokom toplotnom kapacitivnošću, dok su donje površine tih materijala adijabatske. Gornji deo dimnjaka razmatrane solarne elektrane je rezervoar oblika šupljeg cilindra koji najviše toplote prima od strane rotirajućih ogledala. Takođe je izvršeno upoređenje predloženog modela sa prototipom klasične solarne dimnjačke elektrane.

SOLARNA DIMNJAČKA ELEKTRANA OBLIKA PIRAMIDE SA KVADRATNOM OSNOVOM: TEORIJSKA RAZMATRANJA

Dardan Klimenta, Joan Peuteman i Jelena Klimenta